Supplemental Material

Methods:

Animals.

Tsp4$^{+/-}$ mice were obtained from The Jackson Laboratory and bred in our facility. From these, *tsp4*$^{-/-}$ and littermate controls (*tsp4*$^{+/+}$*)* were generated.

The *TSP4* gene was inactivated by replacing 14 nucleotides in the first intron of its genomic sequence with a LacZ-neomycin resistance cassette (Lac0-SA-IRES-lacZNeo555G/Kan). When *TSP4* DNA was analyzed by Southern blots, the recombinant ES cell line showed an additional, single band of the predicted size. The mechanism for the insertional inactivation of *Tsp4* was essentially that of a promoter intron trap in which a splice acceptor sequence was fused 5' to a LacZ-Neo cassette that contained a poly A sequence at its 3' end. As a result, β-galactosidase was expressed under the control of the endogenous *Tsp4* promoter and the *Tsps4* gene was silenced. Homologous recombination in the ES cell line used to generate the TSP-4-null mouse was verified by 3'PCR and 5' Southern blot analysis of genomic DNA (for additional information go to: http://jaxmice.jax.org/strain/005845.html). *Tsp4*$^{-/-}$ mice were backcrossed onto a C57BL/6 background for 12 generations. The absence of cardiac TSP4 mRNA was confirmed by Northern blots (Fig 1B). 10-12 week-old *tsp4*$^{-/-}$ and littermate controls (*tsp4*$^{+/+}$*)* were used for all experiments. All animal procedures were performed according to NIH guidelines under protocols approved by the Institutional Animal Care and Use Committee of the Johns Hopkins University.

Trans-aortic constriction.

Mice were anesthetized with isoflurane (3%), the chest opened through a small thoracic window between ribs 2 and 4, and a 26 G needle placed on the transverse aorta as described[1]. This needle size was chosen to elicit a moderate response as initial studies using our standard TAC model (27 G needle) led to increased mortality in *tsp*$^{-/-}$ mice. The band was secured using a 7.0 prolene suture, the needle was then removed and the chest closed. Animals were allowed to recover and returned to the animal facility.

Echocardiographic evaluation. *In vivo* cardiac geometry and function were serially assessed by transthoracic echocardiography (Acuson Sequoia C256, 13 MHz transducer; Siemens) in conscious mice. M-mode LV end-systolic and end-diastolic cross-sectional diameter (LVESD, LVEDD), and the mean of septal and posterior wall thicknesses were determined from an average of 3–5 cardiac cycles. LV fractional shortening (%FS) and LV mass were determined using a cylindrical model.

Trabeculae experiments:

10-12 week-old male *tsp4*$^{+/+}$ and *tsp4*$^{-/-}$ mice were anesthetized with inhaled isoflurane, and then cervically dislocated. The heart was quickly excised and placed in modified Krebs-Henseleit (KH) solution containing 30 mmol/L 2,3-butadione monoxime (BDM). The KH solution contained (in mM) 141 NaCl, 50 Dextrose, $NaHCO_3$, 5 HEPES, 5 KCl, 1.2 NaH_2PO_4, 1 $MgSO_4$ and 2.0 CaCl, pH adjusted to 7.35, and bubbled with 95% O_2, 5% CO_2. Thin papillary muscle strips of similar shape and size were dissected from the right ventricle. Force and calcium were simultaneously measured as described previously[2]. Muscle was studied at 27^{o}C perfused with KH solution, and field stimulated at 0.5 Hz. Force was measured using a force transducer (Scientific Instruments GmbH, Heidleberg, Germany). Calcium transients were measured using

the fluorescent dye fura-2AM (Invitrogen). The muscle was diffusionally loaded for 30 minutes, dye excited at 340 nm and 380 nm, and emitted fluorescence measured at 510 nm using a photomultiplier tube (R1527, Hamamatsu, Japan). The ratio of fluorescence emission from 340 nm excitation and 380 nm excitation, *R*, was calculated after subtracting background fluorescence. The length at maximal force L_{max} was established, and then reduced to 92%. After steady state, the muscle was stretched from 92%-98%L_{max}, and force and calcium simultaneously recorded over the ensuing 10 minutes. In a second set of experiments, muscles were pre-treated for 15 minutes with 400 pM recombinant human TSP4 (R&D Systems, Minneapolis, MN), and the slow force response was measured.

Myocyte Isolation and Physiologic Analysis

Adult cardiac myocytes were freshly isolated from *tsp4*$^{-/-}$ mice and from littermate (WT) controls as described[3]. Briefly, hearts were quickly removed from the chest after euthanasia and the aorta retroperfused at 100 cmH_2O and 37ºC for ~3 min with a Ca^{2+}-free bicarbonate-based buffer, gassed with 95% O_2-5% CO_2. Following enzymatic digestion, dispersed myocytes were filtered through a 150 µm mesh and gently centrifuged at 500 rpm for 30 seconds. The pellet was re-suspended in Tyrode's solution with increasing Ca^{2+} (1 mM), and cells then incubated for 15 min with 3 µmol/l Fura2-AM (Invitrogen, Molecular Probes, Carlsbad CA) in Tyrodes (1 mM Ca^{2+}). After rinsing, cells were placed in a perfusion chamber with a flow-through rate of 2 ml/min, and sarcomere length and whole cell Ca^{2+} transients recorded using an inverted fluorescence microscope (Nikon, TE2000), and IonOptix (Myocam®) software.

Force-length measurements. The single cardiomyocyte force-length measurement system has been described by Nishimura *et al.*[4]. Briefly, a rod-shaped quiescent single cardiomyocyte was selected under a microscope and a pair of carbon fibers was attached to both ends using

micromanipulators. Two compliant fibers were used, each digitally controlled by piezoelectric translator (Physik Instrumente, P-841-80). Cells were electrically stimulated at 0.2 Hz with 15-ms pulses. Cardiomyocyte sarcomere length and carbon fiber tip displacements were recorded at 120 Hz and analyzed in real time using IonOptix (MA) equipment and software. Cells were stretched to 105% of slack length for the studies, and active and passive force (F) determined from fiber bending given by $F = K(DL_P\text{-}DL_F)$, where K is the effective stiffness of the compliant carbon fiber, DL_F is the change in distance between the two carbon fibers, and DL_P is the displacement of piezoelectric translator.

Neonatal stretched myocytes experiments: Rat neonatal cultured cardiomyocytes were stretched on a Flexcell system. Myocytes were plated on a flexible silastic-bottom dish and subjected to 10% cyclic stretch (1Hz).Supernatant (media) was aspirated, and trizol reagent was added to extract total RNA. RT-PCR was then performed.

Western Blot Analysis: Snap frozen heart tissues were homogenized in cell lysis buffer (Cell Signaling Technology, Danvers, MA) with 0.01% phosphatase inhibitors (Sigma, St. Louis, MO) and protease inhibitor PMSF (10 mM, Roche, Nutley, NJ). 60 µg protein was loaded onto 8–16% Tris–Glycine Novex mini-gels (Invitrogen, Carlsbad, CA), electrophoresed and transferred to nitrocellulose or PDVF membranes. Primary antibodies were Akt: 1:1000, p-Akt: 1:250, ERK: 1:1000, p-ERK: 1:1000 (Cell Signaling, Danvers, MA).

Microarray analysis: Hearts from $tsp4^{-/-}$ and $tsp4^{+/+}$ (n= 4 each) were rapidly explanted and frozen in liquid nitrogen. Illumina's MouseRef-8 v2.0 Expression BeadChip arrays were used, which target approximately 25,600 well-annotated RefSeq transcripts, over 19,100 unique genes, and enable the interrogation of eight samples in parallel (4 wild-type and 4 TSP-4 knock-out mice). Microarray data were normalized using quantile normalization implemented in Bioconductor's “affy”-package (www.bioconductor.org). To determine differentially expressed

genes, unpaired two-class Significance Analysis of Microarrays (SAM) was used (5). Functional annotation of differentially expressed genes was based on the Kyoto Encyclopedia of Genes and Genomes (KEGG) pathways (6), implemented in the Database for Annotation, Visualization and Integrated Discovery (DAVID) (7).

Histology and interstitial fibrosis determination: Myocardial fibrosis was determined from Masson trichrome stained paraffin-embedded myocardial sections, examined using standard as well as polarized light illumination. A total of 4 slides from each heart, from a total of 5 hearts from each group were analyzed. All slides were scored by an expert operator blinded to tissue source using a semi-quantitative scale (0=absent; 3=marked fibrosis).

Figure legends.

Figure S1. Baseline cardiac function and morphology. (**A**). Representative left ventricular pressure-volume loops from tsp4+/+ and tsp4-/- mice. These were similar between genotypes. (**B**). Summary data for resting heart rate (HR), systolic blood pressure (SBP), dP/dtmax, and left ventricular ejection fraction (EF). (**C**). Summary data based on echocardiography showing similar baseline LV fractional shortening (FS), end-diastolic dimension (EDD), end-systolic dimension (ESD), and left ventricular wall thickening (WT).

Table S2. Heart rate (HR), systolic blood pressure (SBP), left ventricular end-diastolic pressure (LVEDP), cardiac output (CO), dP/dtmax, and Tau (relaxation constant) were similar between *tsp4+/+* and *tsp4 -/-* mice

Figure S2. Example time-tracings and summary results for cardiomyocyte sarcomere shortening and calcium transients in tsp4+/+ and tsp4-/- cells. Both had similar function and Ca2+ transients at rest and after isoproterenol (ISO, 10nM) stimulation. # = $p<0.01$ compared to baseline.

Figure S3. Left ventricular systolic pressure (LVSP) measured at baseline and 15 minutes after TAC was performed in $tsp4^{+/+}$ and $tsp4^{-/-}$ mice. TAC imposed a similar initial cardiac workload to both strains. N= 6 in each group.

Supplemental data references.

1. Cingolani OH, Perez NG, Ennis IL, Alvarez MC, Mosca SM, Schinella GR, Escudero EM, Console G, Cingolani HE. In vivo key role of reactive oxygen species and nhe-1 activation in determining excessive cardiac hypertrophy. *Pflugers Archiv : European journal of physiology*. 2011

2. Kirk JA, MacGowan GA, Evans C, Smith SH, Warren CM, Mamidi R, Chandra M, Stewart AF, Solaro RJ, Shroff SG. Left ventricular and myocardial function in mice

expressing constitutively pseudophosphorylated cardiac troponin i. *Circ Res*. 2009;105:1232-1239

3. Lee DI, Vahebi S, Tocchetti CG, Barouch LA, Solaro RJ, Takimoto E, Kass DA. Pde5a suppression of acute beta-adrenergic activation requires modulation of myocyte beta-3 signaling coupled to pkg-mediated troponin i phosphorylation. *Basic Res Cardiol*. 2010;105:337-347

4. Nishimura S, Yasuda S, Katoh M, Yamada KP, Yamashita H, Saeki Y, Sunagawa K, Nagai R, Hisada T, Sugiura S. Single cell mechanics of rat cardiomyocytes under isometric, unloaded, and physiologically loaded conditions. *Am J Physiol Heart Circ Physiol*. 2004;287:H196-202.

5. Tusher VG, Tibshirani R, Chu G. Significance analysis of microarrays applied to the ionizing radiation response. Proc.Natl.Acad Sci U.S.A. 2001;98:5116-5121.

6. Dennis G, Jr., Sherman BT, Hosack DA, Yang J, Gao W, Lane HC, Lempicki RA. DAVID: Database for Annotation, Visualization, and Integrated Discovery. Genome Biol. 2003;4:P3.

7. Kanehisa M, Goto S. KEGG: Kyoto Encyclopedia of Genes and Genomes. Nucleic Acids Res. 2000;28:27-30.

Online Table I. Downregulated Genes (10% false positive rate)

ACSL5	acyl-CoA synthetase long-chain family member 5
ACTN1	actinin, alpha 1
ADAMTS2	a disintegrin-like and metallopeptidase (reprolysin type) with thrombospondin type 1 motif, 2; similar to A disintegrin-like and metallopeptidase (reprolysin type) with thrombospondin type 1 motif, 2
ADCY4	adenylate cyclase 4
AGPAT6	1-acylglycerol-3-phosphate O-acyltransferase 6 (lysophosphatidic acid acyltransferase, zeta)
ANTXR1	anthrax toxin receptor 1
ANXA2	similar to Annexin A2 (Annexin II) (Lipocortin II) (Calpactin I heavy chain) (Chromobindin-8) (p36) (Protein I) (Placental anticoagulant protein IV) (PAP-IV); annexin A2
ANXA3	similar to Anxa3; annexin A3
AOC3	amine oxidase, copper containing 3
ARHGEF3	Rho guanine nucleotide exchange factor (GEF) 3
ARMCX1	armadillo repeat containing, X-linked 1
ARMCX2	armadillo repeat containing, X-linked 2
ASB2	ankyrin repeat and SOCS box-containing 2
ASPN	asporin
ASS1	argininosuccinate synthetase 1
ATOX1	ATX1 (antioxidant protein 1) homolog 1 (yeast)
ATP5K	predicted gene 2972; ATP synthase, H+ transporting, mitochondrial F1F0 complex, subunit e
ATP6AP1	ATPase, H+ transporting, lysosomal accessory protein 1
AURKA	aurora kinase A
AW555464	expressed sequence AW555464
BACE2	beta-site APP-cleaving enzyme 2
BC004728	N/A
BC028528	cDNA sequence BC028528
BCL11B	B-cell leukemia/lymphoma 11B
BGN	biglycan
BMP1	bone morphogenetic protein 1
BOK	BCL2-related ovarian killer protein
CACNA1G	calcium channel, voltage-dependent, T type, alpha 1G subunit
CCND1	cyclin D1
CD34	CD34 antigen
CD40	CD40 antigen
CD97	CD97 antigen
CDC42EP2	CDC42 effector protein (Rho GTPase binding) 2
CENPT	centromere protein T

CHST7	carbohydrate (N-acetylglucosamino) sulfotransferase 7
CKB	similar to creatine kinase, brain; predicted gene 12892; creatine kinase, brain
CLIC1	chloride intracellular channel 1
CLTA	clathrin, light polypeptide (Lca)
COL15A1	collagen, type XV, alpha 1
COL16A1	collagen, type XVI, alpha 1
COL18A1	collagen, type XVIII, alpha 1
COL1A1	collagen, type I, alpha 1
COL4A1	collagen, type IV, alpha 1
COL5A1	collagen, type V, alpha 1
COL6A1	collagen, type VI, alpha 1
COL6A2	collagen, type VI, alpha 2
CORO1C	coronin, actin binding protein 1C; predicted gene 5790
COX7A2	cytochrome c oxidase, subunit VIIa 2
CPA3	carboxypeptidase A3, mast cell
CSRP2	cysteine and glycine-rich protein 2
CTNNBIP1	catenin beta interacting protein 1
CXADR	coxsackie virus and adenovirus receptor
D630003M21RIK	RIKEN cDNA D630003M21 gene
DAB2IP	disabled homolog 2 (Drosophila) interacting protein
DDAH1	dimethylarginine dimethylaminohydrolase 1
DGCR2	DiGeorge syndrome critical region gene 2
DNAJA3	DnaJ (Hsp40) homolog, subfamily A, member 3
DOK4	docking protein 4
DPYSL2	dihydropyrimidinase-like 2
DTNA	dystrobrevin alpha
E2F1	E2F transcription factor 1
EDF1	predicted gene 11964; endothelial differentiation-related factor 1
ENDOD1	endonuclease domain containing 1
ENTPD2	ectonucleoside triphosphate diphosphohydrolase 2
EPHB1	Eph receptor B1
ERP29	endoplasmic reticulum protein 29
F8	coagulation factor VIII
FABP5	fatty acid binding protein 5, epidermal
FAM129B	family with sequence similarity 129, member B
FIGNL1	fidgetin-like 1
FSCN1	fascin homolog 1, actin bundling protein (Strongylocentrotus purpuratus)
FSTL1	follistatin-like 1
FXYD5	FXYD domain-containing ion transport regulator 5

GMCL1	germ cell-less homolog 1 (Drosophila)
GNAI2	guanine nucleotide binding protein (G protein), alpha inhibiting 2; similar to Guanine nucleotide-binding protein G(i), alpha-2 subunit (Adenylate cyclase-inhibiting G alpha protein)
GPC3	glypican 3
GPX7	glutathione peroxidase 7
GRASP	GRP1 (general receptor for phosphoinositides 1)-associated scaffold protein
H2-AB1	histocompatibility 2, class II antigen A, beta 1; response to metastatic cancers 2; similar to H-2 class II histocompatibility antigen, A-D beta chain precursor
HCN2	hyperpolarization-activated, cyclic nucleotide-gated K+ 2
HMGN3	high mobility group nucleosomal binding domain 3
HN1	hematological and neurological expressed sequence 1; predicted gene 3687
HRMT1L2 = PRMT1	protein arginine methyltransferase 1
HSD3B5	hydroxy-delta-5-steroid dehydrogenase, 3 beta- and steroid delta-isomerase 5
HYAL2	hyaluronoglucosaminidase 2
ICAM2	intercellular adhesion molecule 2
IFT122	intraflagellar transport 122 homolog (Chlamydomonas)
IGF2	insulin-like growth factor 2
IL16	interleukin 16
IQGAP2	IQ motif containing GTPase activating protein 2
ITPK1	inositol 1,3,4-triphosphate 5/6 kinase
ITPR2	inositol 1,4,5-triphosphate receptor 2
KCNAB2	potassium voltage-gated channel, shaker-related subfamily, beta member 2
KCNK6	potassium inwardly-rectifying channel, subfamily K, member 6
KDELR3	KDEL (Lys-Asp-Glu-Leu) endoplasmic reticulum protein retention receptor 3
KNG2	kininogen 2
LAPTM5	lysosomal-associated protein transmembrane 5
LASP1	LIM and SH3 protein 1
LIMS2	LIM and senescent cell antigen like domains 2
LMNB2	lamin B2
LOC100038882	N/A
LOC100041504	predicted gene 13304; similar to beta chemokine Exodus-2; predicted gene 10591; chemokine (C-C motif) ligand 21B; chemokine (C-C motif) ligand 21C (leucine)
LOC100042777	N/A
LOC100047167	similar to mKIAA0990 protein; chondroitin sulfate synthase 1
LOC100047856	similar to calponin 3, acidic; predicted gene 4815; calponin 3, acidic
LOC100048710	hypothetical protein LOC100048710
LRRK1	leucine-rich repeat kinase 1
LRRN1	leucine rich repeat protein 1, neuronal

LXN	latexin
MAF1	MAF1 homolog (S. cerevisiae)
MAZ	MYC-associated zinc finger protein (purine-binding transcription factor)
MCF2L	mcf.2 transforming sequence-like
MCM6	minichromosome maintenance deficient 6 (MIS5 homolog, S. pombe) (S. cerevisiae)
MDM2	transformed mouse 3T3 cell double minute 2
ME3	malic enzyme 3, NADP(+)-dependent, mitochondrial
MFAP5	microfibrillar associated protein 5
MGP	matrix Gla protein
MMP2	matrix metallopeptidase 2
MRGPRF	MAS-related GPR, member F
MRPS25	mitochondrial ribosomal protein S25
MRPS27	mitochondrial ribosomal protein S27
MTCH1	mitochondrial carrier homolog 1 (C. elegans)
MYO9B	myosin IXb
NANS	N-acetylneuraminic acid synthase (sialic acid synthase)
NCKAP1L	NCK associated protein 1 like
NDN	necdin
NOTCH4	Notch gene homolog 4 (Drosophila)
NUAK1	NUAK family, SNF1-like kinase, 1
NUDT18	nudix (nucleoside diphosphate linked moiety X)-type motif 18
NUPR1	nuclear protein 1
OLFR1449	olfactory receptor 1449
PACSIN3	protein kinase C and casein kinase substrate in neurons 3
PALM	paralemmin
PBX2	pre B-cell leukemia transcription factor 2
PDGFRL	platelet-derived growth factor receptor-like
PEMT	phosphatidylethanolamine N-methyltransferase
Pf4 = CXCL4	platelet factor 4
PGD	phosphogluconate dehydrogenase
PIP4K2A	phosphatidylinositol-5-phosphate 4-kinase, type II, alpha
PMP22	peripheral myelin protein 22
PON2	paraoxonase 2
PPM1F	protein phosphatase 1F (PP2C domain containing)
PPP1R3C	protein phosphatase 1, regulatory (inhibitor) subunit 3C
PPP2R5C	protein phosphatase 2, regulatory subunit B (B56), gamma isoform
PPP4R1	protein phosphatase 4, regulatory subunit 1
PRCP	prolylcarboxypeptidase (angiotensinase C)
PRKCD	protein kinase C, delta

PRR13	proline rich 13
PSMB10	proteasome (prosome, macropain) subunit, beta type 10
PSME1	predicted gene 7776; proteasome (prosome, macropain) 28 subunit, alpha
PTGIS	prostaglandin I2 (prostacyclin) synthase
PTPN6	protein tyrosine phosphatase, non-receptor type 6
PYGO2	pygopus 2
RAB31	RAB31, member RAS oncogene family
RAMP1	receptor (calcitonin) activity modifying protein 1
RBM47	RNA binding motif protein 47
RDH5	retinol dehydrogenase 5
RHOC	ras homolog gene family, member C
RIN3	Ras and Rab interactor 3
RNF19A	ring finger protein 19A
RPL27A	predicted gene 14439; predicted gene 8213; predicted gene 13981; predicted gene 8451; predicted gene 6378; predicted gene 8667; predicted gene 4923; predicted gene 5908; ribosomal protein L27a; predicted gene 14044; predicted gene 7536; predicted gene 14407
RPS6KL1	ribosomal protein S6 kinase-like 1
RRBP1	ribosome binding protein 1
RTN1	reticulon 1
SAE1	SUMO1 activating enzyme subunit 1
SAMD9L	sterile alpha motif domain containing 9-like
SCARF2	scavenger receptor class F, member 2
SCD1	stearoyl-Coenzyme A desaturase 1
SCN1B	sodium channel, voltage-gated, type I, beta
SDC3	syndecan 3
SEC61B	Sec61 beta subunit; predicted gene 10320; predicted gene 5870; similar to protein translocation complex beta subunit predicted gene 11575; predicted gene 10177; predicted gene 4184; SEC61, gamma subunit; similar to Sec61-complex
SEC61G	gamma-subunit
SEMA3F	sema domain, immunoglobulin domain (Ig), short basic domain, secreted, (semaphorin) 3F
SENP6	similar to Sentrin-specific protease 6 (Sentrin/SUMO-specific protease SENP6) (SUMO-1-specific protease 1); SUMO/sentrin specific peptidase 6
SERF2	small EDRK-rich factor 2
SGOL1	shugoshin-like 1 (S. pombe)
SH3PXD2B	SH3 and PX domains 2B
SIRPA	signal-regulatory protein alpha
SLC25A19	solute carrier family 25 (mitochondrial thiamine pyrophosphate carrier), member 19
SLC9A3R2	solute carrier family 9 (sodium/hydrogen exchanger), member 3 regulator 2
SMAD1	MAD homolog 1 (Drosophila)
SRPK3	serine/arginine-rich protein specific kinase 3

ST6GALNAC2	ST6 (alpha-N-acetyl-neuraminyl-2,3-beta-galactosyl-1,3)-N-acetylgalactosaminide alpha-2,6-sialyltransferase 2
ST7L	suppression of tumorigenicity 7-like
STXBP4	syntaxin binding protein 4
SUV420H2	suppressor of variegation 4-20 homolog 2 (Drosophila)
TDRD7	tudor domain containing 7
TGFBI	transforming growth factor, beta induced
TIMELESS	timeless homolog (Drosophila)
TMEM119	transmembrane protein 119
TMEM51	transmembrane protein 51
TMSB10	predicted gene 3787; predicted gene 9844; predicted gene 8034; similar to thymosin, beta 10; thymosin, beta 10
TSPAN2	tetraspanin 2
TUBB2B	tubulin, beta 2a, pseudogene 2; tubulin, beta 2B
TUBB5	tubulin, beta 5
UHRF2	ubiquitin-like, containing PHD and RING finger domains 2
UNC13B	unc-13 homolog B (C. elegans)
VIM	vimentin
VKORC1	vitamin K epoxide reductase complex, subunit 1
VPS4A	vacuolar protein sorting 4a (yeast)
WFDC1	WAP four-disulfide core domain 1
XPNPEP1	X-prolyl aminopeptidase (aminopeptidase P) 1, soluble
YWHAB	tyrosine 3-monooxygenase/tryptophan 5-monooxygenase activation protein, beta polypeptide
YWHAQ	predicted gene, EG546165; predicted gene 2423; hypothetical protein LOC674211; tyrosine 3-monooxygenase/tryptophan 5-monooxygenase activation protein, theta polypeptide
ZFP282	zinc finger protein 282

Upregulated Genes (10 % False Discovery Rate)

A2BP1	ataxin 2 binding protein 1
AMY1	amylase 1, salivary
CIRBP	cold inducible RNA binding protein
CP	ceruloplasmin
GRB14	growth factor receptor bound protein 14
IDE	insulin degrading enzyme
L2HGDH	L-2-hydroxyglutarate dehydrogenase; predicted gene 7842
POPDC2	popeye domain containing 2
RBPMS	RNA binding protein gene with multiple splicing
RETSAT	retinol saturase (all trans retinol 13,14 reductase)
SORD	sorbitol dehydrogenase

Annotation Cluster 1	**Enrichment Score: 6.09**	
SP_PIR_KEYWORDS	extracellular matrix	**RT**
GOTERM_CC_FAT	proteinaceous extracellular matrix	**RT**
GOTERM_CC_FAT	extracellular matrix	**RT**
Annotation Cluster 2	**Enrichment Score: 4.58**	
SP_PIR_KEYWORDS	hydroxylation	**RT**
INTERPRO	Collagen triple helix repeat	**RT**
SP_PIR_KEYWORDS	collagen	**RT**
Annotation Cluster 3	**Enrichment Score: 2.94**	
GOTERM_BP_FAT	cell adhesion	**RT**
GOTERM_BP_FAT	biological adhesion	**RT**
SP_PIR_KEYWORDS	cell adhesion	**RT**
Annotation Cluster 4	**Enrichment Score: 2.71**	
UP_SEQ_FEATURE	region of interest:Triple-helical region	**RT**
GOTERM_MF_FAT	platelet-derived growth factor binding	**RT**
GOTERM_CC_FAT	collagen	**RT**
GOTERM_MF_FAT	growth factor binding	**RT**

Online Table II

	HR (1/min)	SBP (mmHg)	LVEDP (mmHg)	CO (µL/min)	dP/dtmax (mmHg/sec)	dP/dt/IP (1/sec)	Tau(G) (msec)
Tsp4 +/+	495 ± 44	89.3 ± 2	7.3 ± 0.9	12.3 ± 1.3	10179 ± 988	189 ± 14	8.2 ± 0.7
Tsp4 -/-	516 ± 29	93.6 ± 5	6.7 ± 0.5	10 ± 0.9	11175 ± 889	218 ± 13	9.1 ± 0.4

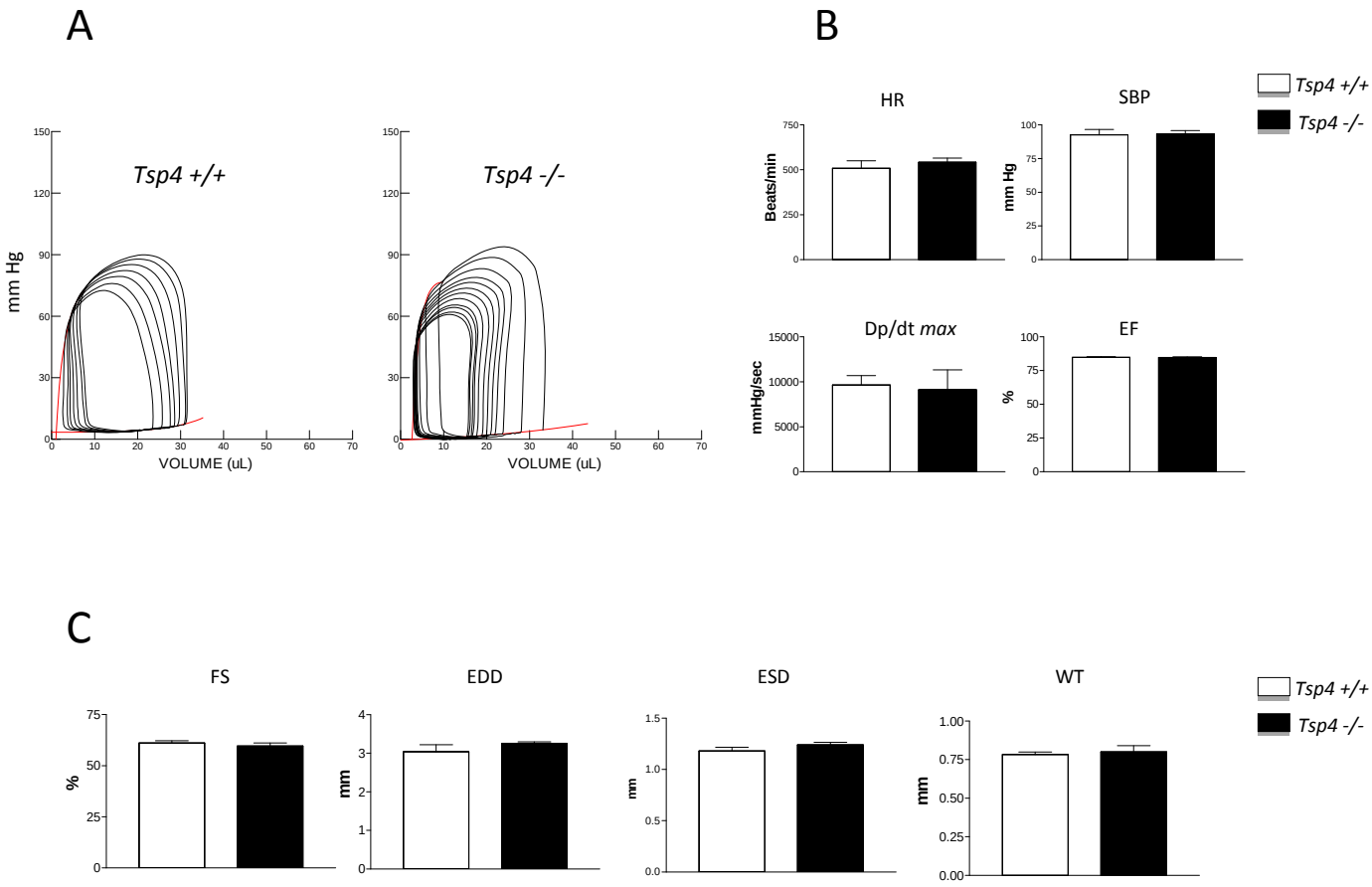

Online Figure I

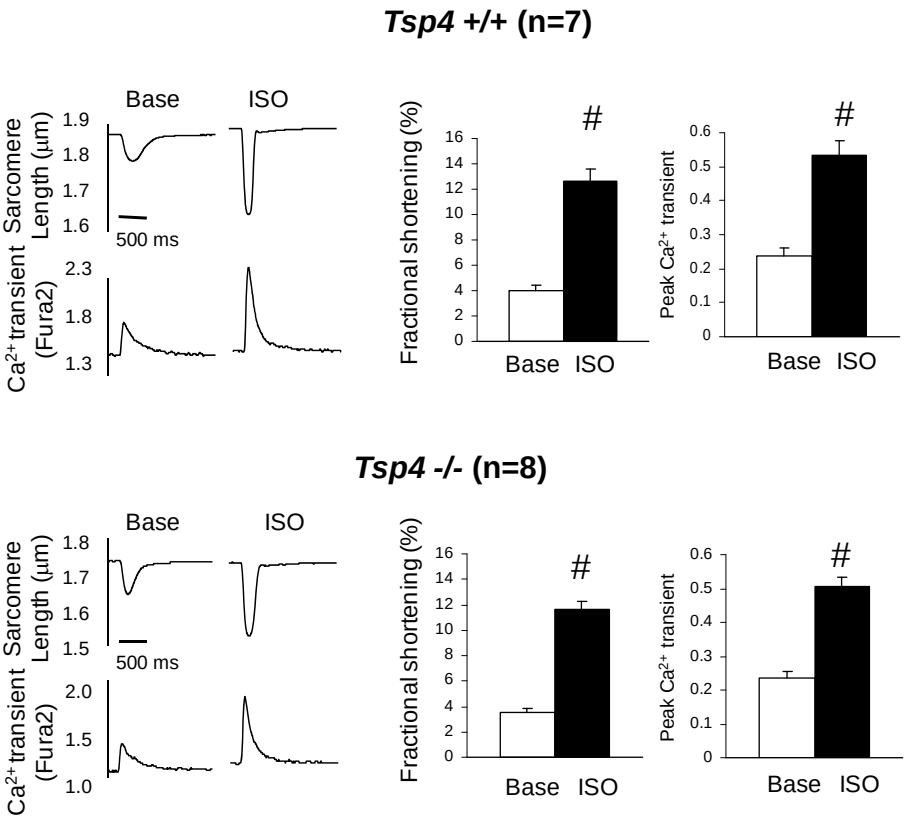

Online Figure II

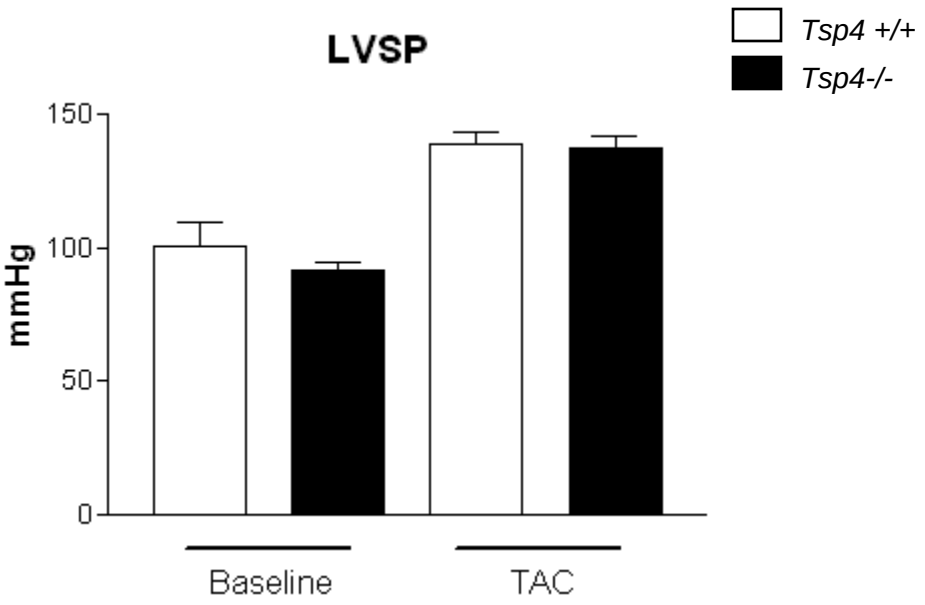

Online Figure III